ENCIT 2018

ABCM Associação Brasileira de Engenharia e Ciências Mecânicas

17th Brazilian Congress of Thermal Sciences and Engineering
November 25th-28th, 2018, Águas de Lindóia, SP, Brazil

ENCIT-2018-0202
MAGNETIZATION DYNAMICS IN FERROFLUIDS: A DYNAMICAL SYSTEM APPROACH

Guilherme Hasse Urel, Rafael Gabler Gontijo*
Universidade Estadual de Campinas, Faculdade de Engenharia Mecânica, Departmento de Energia, Rua Mendeleyev, 200, Unicamp, 13083-970, Campinas - SP, Brazil
guilhermeurel@gmail.com, rafaelgabler@fem.unicamp.br

Francisco Ricardo Cunha*
Universidade de Brasilia, Departamento de Engenharia Mecânica, UnB, 70910-900, Brasilia - DF, Brazil
frcunha2@gmail.com

*Vortex Group- Fluid Mechanics of Complex Flows

Abstract. *This work presents a numerical study of the magnetization dynamics of magnetic fluids. The problem is governed by a nonlinear ordinary differential phenomenological equation that considers three mechanisms: the influence of vorticity, a relaxation magnetic process and a restorative magnetic mechanism associated with an external field. The problem is explored in terms of a dynamical system using time and frequency signatures and phase-space diagrams. Each mechanism is isolated, investigated and physically discussed. We identify a demagnetization mechanism associated with the flow vorticity and a restorative effect of external magnetic torques. The influence of dipolar long range particle interactions is also modeled by a third order asymptotic theory.*

Keywords: *ferrofluids, magnetization, dynamical systems, phenomenological model, magnetic fluids*

1. INTRODUCTION

A ferrofluid is a stable colloidal suspension of nanosized ferromagnetic particles dispersed in a Newtonian carrier base-fluid, usually water or synthetic oils (Rosensweig, 1985). In the absence of an external magnetic field the rheological behavior of these fluids is purely Newtonian, however when subjected to a magnetic field its microstructure is altered in interesting ways from a rheological perspective. The possibility to exert remote control in a fluid using magnetic fields is fascinating. The magnetoviscous effect (MVE), i.e., the viscosity change through the application of an external magnetic field, explored experimentally by Rosensweig (1969) and McTague (1969), is an example of these peculiarities that confer to a magnetic fluids a vast range of applications as presented and discussed by Raj, Boulton and Casciari (1995).

As a motivation for this work some of these applications and studies can be mentioned: Snyder, Cader and Filayson (2002) studied the influence of the magnetic effect in the convectional mechanism; Cunha and Sobral (2004) analyzed an application in the separation between water and oil; Lubbe (2001) and Voltairas (2002) explored drug delivery in targeted therapies; magnetic hyperthermia, a method to treat cancerous tumors through abrupt thermal variation, have been studied by Zubarev (2015) and many others; stabilization of fluidized beds was approached by Cunha, Sobral and Gontijo (2013) and the insertion of magnetic particles in hydraulic machines to attenuate cavitation was studied by Cunha, Souza and Morais (2002). All of these to evidence the wide spectrum of possibilities.

In terms of mathematical formuation, we have an interesting case of a hydrodynamic-magnetic coupling. The stress tensor of a ferrofluid is modified in relation to the Newtonian case. For that reason the fluid motion equation presents terms related to classical vector fields of electromagnetic theory that are not observed otherwise (Odenbach, 2009). These new terms demand additional modeling for closure. The main physical variable for the magnetic-hydrodynamic coupling in Ferrohydrodynamics (FHD) is the magnetization field. This field is ruled by an evolution partial differential equation (PDE). This equation is the subject of this work. The FHD equations can be summarized by conservation laws and Maxwell's equations in one side and a constitutive equation in the other. While the former are derived from basic physical laws, the latter still is an active research field (Larson, 1999).

Many models have already been proposed for the magnetization vector field using several approaches (thermodynamical, microscopical and phenomenological) evidencing its importance in the problem's closure. Using a phenomenological view, Shliomis (1971) proposed a model, used in this work, considering that the magnetization is affected by three mechanisms: vorticity, magnetic relaxation to equilibrium and a restorative field effect that is modeled through a precession term. This model was criticized by Odenbach (2002) over the fact that the influence of vorticity does not distinguish its nature, i.e., if the magnetization deviation is a result of rotation or elongation of flow. Furthermore the influence of interparticle correlations, that are not considered in Shliomis (1971) pioneer model, were incorporated in the present article through the proposal of Ivanov and Kuznetsova (2001) on the equilibrium magnetization.

In order to explore the peculiarities of the magnetization dynamics of ferrofluids we use a dynamical system approach. The full model, that considers the three former mechanisms and the interparticle correlation, is applied here using oscillatory shear and magnetic fields. The role of each physical parameter and the excitation frequencies of the system can be explored and physically interpreted through this method. Interesting phenomenas can be understood optimizing a certain response through the study of the system solutions and the manipulation of physical parameters.

2. FORMULATION OF THE PROBLEM

The magnetization vector field is an average over all the dipoles of the ferromagnetic particles in the colloidal suspension of their alignment in the direction of an external magnetic field. The model proposed by Shliomis (1972) can be summarized through the following differential equation, that computes the temporal derivative of magnetization induced by the flow vorticity and magnetic relaxation an restoration:

$$\frac{d\boldsymbol{M}}{dt} = (\boldsymbol{\Omega} \times \boldsymbol{M}) + \frac{1}{\tau_B}(\boldsymbol{M_0} - \boldsymbol{M}) + \frac{1}{6\eta\phi}\boldsymbol{M} \times (\boldsymbol{H} \times \boldsymbol{M}). \tag{1}$$

Here $\boldsymbol{M}$ stands for the magnetization of the fluid under the flow vorticity $2\boldsymbol{\Omega} = \nabla \times \boldsymbol{u}$ and the external magnetic field $\boldsymbol{H}$, η is the fluid viscosity, $\phi = nV$ is the volumetric fraction of nanoparticles in the suspension, n is their density number, V the volume of a single nanoparticle and $\tau = 3\eta V/k_B T$ is the Brownian time of rotational particle diffusion, where k_B is the Boltzmann constant and T the temperature. In order to incorporate the interparticle correlations according to the model of Ivanov and Kuznetsova (2001), the equilibrium magnetization $\boldsymbol{M_0}$ is given by:

$$\frac{\boldsymbol{M_0}}{\boldsymbol{M_d}} = \mathcal{L}_{(\alpha)}\phi + E_{(\alpha)}\lambda\phi^2 + [F_{(\alpha)} + G_{(\alpha)}]\lambda^2\phi^3, \tag{2}$$

where the functions $\mathcal{L}_{(\alpha)}$, $E_{(\alpha)}$, $F_{(\alpha)}$ and $G_{(\alpha)}$ are:

$$\mathcal{L}_{(\alpha)} = \coth(\alpha) - \frac{1}{\alpha}. \tag{3}$$

$$E_{(\alpha)} = \frac{\pi}{3}\left(\frac{24}{\alpha}\right)\mathcal{L}_{(\alpha)}\left[-\alpha\text{csch}^2_{(\alpha)} + \frac{1}{\alpha}\right] \tag{4}$$

$$F_{(\alpha)} = \frac{1}{2}\left(\frac{\pi}{3}\right)^2\left(\frac{24}{\alpha}\right)^2\mathcal{L}_{(\alpha)}\left[2\alpha^2\text{csch}^2_{(\alpha)}\coth_{(\alpha)} - \frac{2}{\alpha}\right] \tag{5}$$

$$G_{(\alpha)} = \left(\frac{\pi}{12}\right)^2\left(\frac{24}{\alpha}\right)^2\mathcal{L}_{(\alpha)}\left[-\alpha\text{csch}^2_{(\alpha)} + \frac{1}{\alpha}\right]^2 \tag{6}$$

The saturation magnetization is $\boldsymbol{M_s} = \phi\boldsymbol{M_d}$, where $\boldsymbol{M_d}$ is the magnetization of the magnetic particles alone. The parameter $\alpha = \mu_0 mH/k_B T$ is a ratio between an energy of a magnetic field and the Brownian energy and the parameter $\lambda = \mu_0 m^2/\pi k_B T d^3$ is a ratio between an energy of a dipole interaction and the Brownian energy. In these cases μ_0 is the vacuum magnetic permeability, m the dipole moment of the particles and d represents their diameter.

2.1 DIMENSIONLESS EQUATIONS AND PHYSICAL PARAMETERS

In order to establish the problem in conformity with the studies of the area and to make an universal analysis the equation 1, object of study of this work, had to be submitted to a nondimensionalization process through the insertion of the following scales:

$$\boldsymbol{M}^* = \frac{\boldsymbol{M}}{M_s},\ \ \boldsymbol{M_0^*} = \frac{\boldsymbol{M_0}}{M_s},\ \ \boldsymbol{H}^* = \frac{\boldsymbol{H}}{H_0},\ \ t^* = t\dot{\gamma}_0\ \ e\ \ \boldsymbol{\Omega}^* = \frac{1}{\dot{\gamma}_0}\boldsymbol{\Omega}, \tag{7}$$

where M_s is the saturation magnetization, H_0 is a typical value of the magnitude of a magnetic field and $\dot{\gamma}_0$ is a typical value of shear rate. The result of this process is the dimensionless version of the phenomenological equation to the magnetization temporal evolution:

$$\frac{d\boldsymbol{M}}{dt} = (\boldsymbol{\Omega} \times \boldsymbol{M}) + \frac{1}{Pe}(\boldsymbol{M_0} - \boldsymbol{M}) + \frac{3\alpha}{4Pe}\boldsymbol{M} \times (\boldsymbol{H} \times \boldsymbol{M}), \tag{8}$$

here the asterisks have been suppressed to avoid an excessive loading of notation, however all the variables are presented in their dimensionless form. The great gift of this process is the appearance of the Peclet number $Pe = \tau_B\dot{\gamma}$, that can be understood as a ratio between two time scales: one related to a Brownian process and other to the flow, and can be used to explore the physical meanings of the solutions.

2.2 PHYSICAL MODEL: SCHEMATICS

With the intention of analyzing the model details and also the nature of the magnetization field from its solutions, a physical model of reference can be explored using equation 8. In order to make all the mechanisms and parameters covered clear in their application the following schematic is presented:

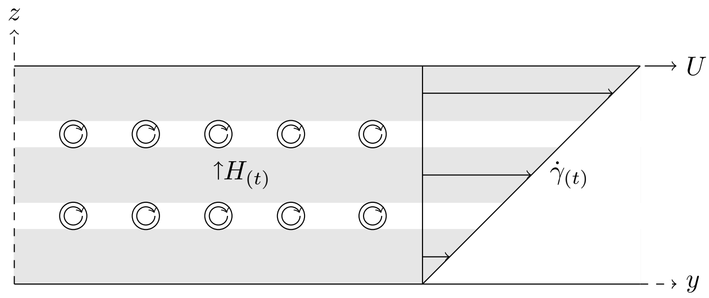

(a) Ferrofluid under a simple shear

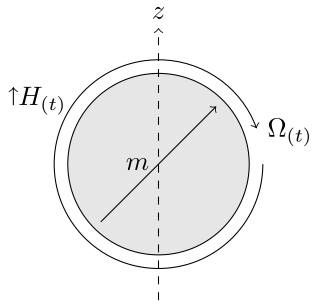

(b) Magnetic particle

Figure 1. Schematic of the physical model of reference.

Figure 1(a) presents a two-dimensional model of ferrofluid under a simple shear with variable shear rate $\dot{\gamma}_{(t)} = \dot{\gamma}_0 \cos(\omega_{\dot{\gamma}} t)$ and variable magnetic field $\boldsymbol{H_{(t)}} = H_0 \cos(\omega_H t)\boldsymbol{\hat{e}_y}$. The white regions represent the role of vorticity in the flow and highlights its influence in the magnetization which is given by: $\boldsymbol{M_{(t)}} = M_{y(t)}\boldsymbol{\hat{e}_y} + M_{z(t)}\boldsymbol{\hat{e}_z}$. Figure 2(b) presents a close of a particle of this ferrofluid under the influences of the vorticity due to $\dot{\gamma}_{(t)}$ and magnetic relaxation and restoration due to $\boldsymbol{H_{(t)}}$. As result of the application of the governing equation to this model is presented the following group of scalar differential equations to be solved:

$$\frac{dM_y}{dt} = -\frac{1}{Pe}M_y - \frac{3\alpha_0}{4Pe}M_z M_y \cos(\omega_H t) + \frac{1}{2}M_z \cos(\omega_{\dot{\gamma}} t) \tag{9}$$

$$\frac{dM_z}{dt} = \frac{1}{Pe}\left(M_0 - M_z\right) + \frac{3\alpha_0}{4Pe}M_y^2 \cos(\omega_H t) - \frac{1}{2}M_y \cos(\omega_{\dot{\gamma}} t) \tag{10}$$

These equations reveal the main parameters of the problem: Pe and $\omega_{\dot{\gamma}}$, related to the vorticity, α_0 and ω_H, related to the magnetic field, λ and ϕ, incorporated in M_0 and related to the interparticle correlations. The analyze of this problem is centered in the influences of each one of these.

3. NUMERICAL METHOD OF SOLUTION

The equations 9 and 10 form a group of coupled nonlinear differential equations that demand an implementation of a numerical method to allow the solution of the full problem (that considers all terms as not null). To accomplish this task a version of an adaptive Runge-Kutta 4-5 method was implemented making use of the Fortran language to a group of input parameters. Furthermore some *MatLab* tools were applied in the post processing of solutions.

4. RESULTS

The system response, i.e., the time series of magnetization can be divided according to the model and the input parameters considered, facilitating the physical interpretation and discussion of each mechanism. In this paper three models are considered: relaxation model, full model and full model with interparticle correlations consideration. Aiming to explore properly some of the features of the system response, time and frequency signatures and phase-space diagrams were also applied.

4.1 RELAXATION MODEL WITH STATIONARY MAGNETIC AND SHEAR FIELDS

The second term of equation 8, $(\boldsymbol{M_0} - \boldsymbol{M})/Pe$, describes the role of magnetic relaxation mechanism, i. e., the restoration of $\boldsymbol{M}$ in the direction of $\boldsymbol{M_0}$. This mechanism can be understood despising the other terms of the equation and exploring its isolated contribution:

$$\frac{dM_z}{dt} = \frac{1}{\tau}(M_0 - M_z), \tag{11}$$

with analytical solution:

$$\frac{M_z}{M_0} = 1 - \exp\left(\frac{-t}{\tau}\right). \tag{12}$$

In the absence of shear the nondimensionalization process is modified, justifying the appearance of τ instead of Pe. With the consideration of the magnetic field and shear rate as stationary, the group of parameters that influence the magnetization dynamics in this case is reduced to τ and α_0 (embedded in $\boldsymbol{M_0}$).

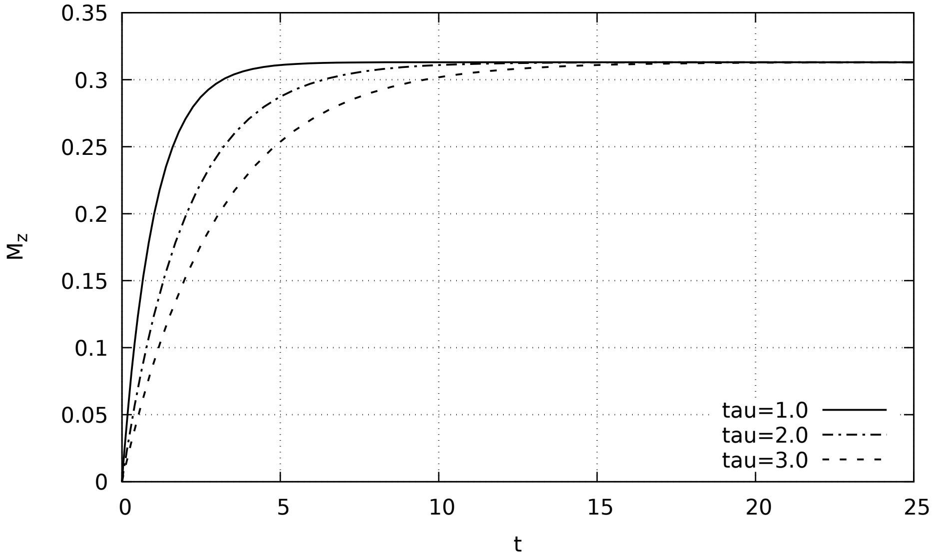

Figure 2. Comparative solution of equation 12 for diverse τ and $\alpha_0 = 1$.

Figure 2 shows how the parameter τ, an analog of Pe, plays the role of the system time constant, governing the velocity of its response and saturation, but not the saturation limit. Established as a ratio between a time scale of a Brownian process and a time scale of a macroscopic one, a low τ value is result of an intense Brownian process (which is processed in a short time) that, due to its probabilistic nature, favors new configurations. In contrast, a high τ value is result of the predominance of a macroscopic effect that confers to the fluid a kind of memory slowing down the formation of new configurations due to the previous ones.

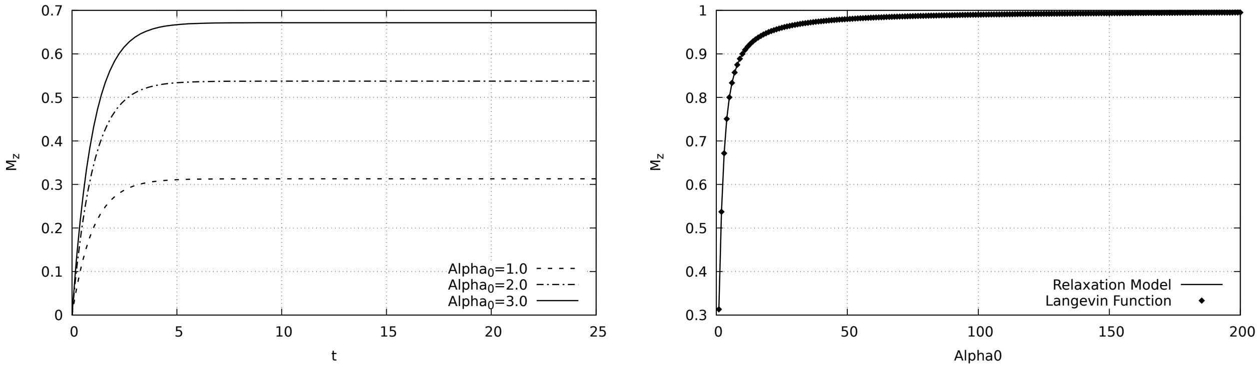

(a) Comparative solution of equation 12 for diverse α_0 and $Pe = 1$.

(b) Saturation limit as function of α_0.

Figure 3. Influence of α_0 in the magnetization dynamics.

The parameter α_0, established as a ratio between the energy of the magnetic field and the Brownian energy, govern the saturation limit of magnetization as showed by Fig. 3. A high α_0 value is result of an intense magnetic field that forces the alignment of magnetic particles, overcoming the Brownian processes and approximating magnetization of its theoretical limit, by definition: $M = 1$.

4.2 FULL MODEL WITH STATIONARY MAGNETIC AND SHEAR FIELDS

The full model, represented by equations 9 and 10 in the limit $\omega_H = \omega_{\dot{\gamma}} = 0$, is the result of adding the influence of vorticity and magnetic restoration to the relaxation model. This equation can be understood as a competition of two mechanisms around a third one, i.e., the flow vorticity and magnetic restoration try to divert the magnetization from its value of relaxation. As result of the insertion of these mechanisms the system response is affected as showed by Fig. 4.

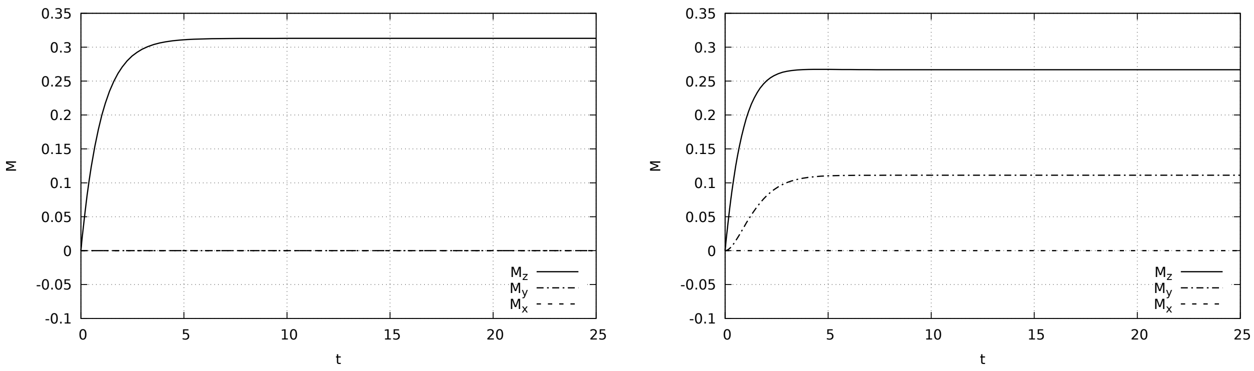

(a) Relaxation model (b) Full model

Figure 4. Comparison between the two models for the following group of input parameters: $Pe = 1$ and $\alpha_0 = 1$

The flow vorticity describes the local spinning motion of a continuum, which can be understood in the scale of the nanoparticles. With this consideration the vorticity could induce the rotational movement of the magnetic particles and their dipoles. Assuming a certain alignment of these, as presented in the relaxation model, the insertion of vorticity, that exerts similar influence in all particles in this kind of flow, justifies the appearance of M_y and the decline of M_z as a simple rotation of the magnetization vector. In order to understand this mechanism we plot in Fig. 5 the relative angle between the components M_z and M_y, defined by $\theta = \text{atan}(M_z/M_y)$ as a function of time for different values of Pe:

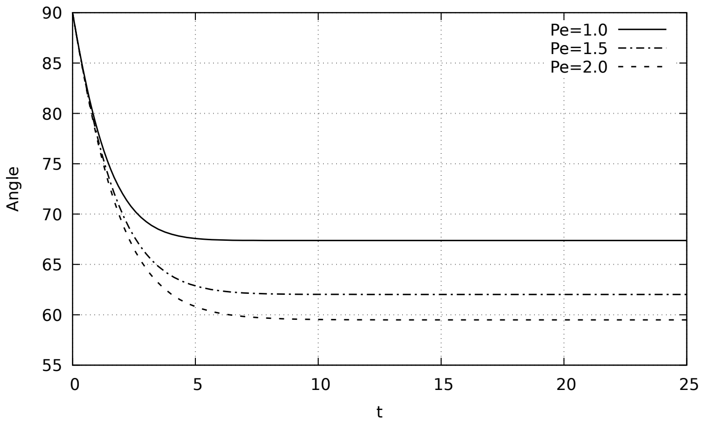

Figure 5. Angle of inclination between $\boldsymbol{M}$ and y axis for $\alpha_0 = 1$ and diverse Pe.

Figure 5 shows a decrease of the magnetization vector in the direction of the applied field due to the increase of Pe, which is the physical parameter that computes the intensity of the rotational effect caused by the shear rate. In order to extrapolate this analysis and comprehend the full relation between magnetization and vorticity, Fig. 6 presents the saturation limits of $\boldsymbol{M}$ as a function of Pe:

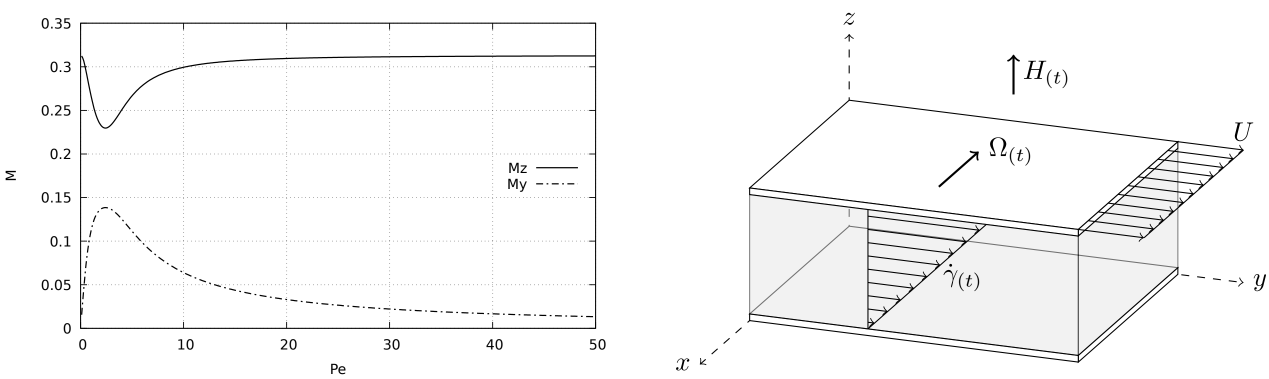

(a) Saturation limits as function of Pe for $\alpha_0 = 1$ (b) 3D schematics of the problem

Figure 6. Figure (a) shows the behavior of the magnetization components as a function of Pe. Figure (b) is an schematics that shows the 3D feature of the problem explored here in the limit $Pe \gg 1$.

The analysis of Fig. 6(a) indicates that the vorticity demagnetization effect reaches a maximum around $Pe \approx 2$, in other words, the inclination of the magnetization vector has a limit. From equation 8 it is possible to notice that in the limit $Pe \to \infty$ the steady state solution for the magnetization field establishes that $\boldsymbol{\Omega} \times \boldsymbol{M} = \boldsymbol{0}$. Since we consider a 2D shear flow, our vorticity $\boldsymbol{\Omega}$ is in the the direction x. This means that in the asymptotic limit $Pe \to \infty$ the magnetization dynamics can no longer be depicted by a 2D model and needs to be treated three dimensionally. The anomalous behavior presented in Fig.6 for $Pe > 2$ is an indication of this phenomenon.

Nevertheless, it is important to notice that Pe is not the only physical parameter responsible for this behavior. Figs. 7 (a) and (b) show the behavior explored in figure 6, for different values of α_0. We observe a displacement in Pe of the maximum and minimum values of M_y and M_z respectively as we increase α_0. This is an indication that the energy of the magnetic field modifies the equivalent particles relaxation Brownian time scale in this magnetization dynamics.

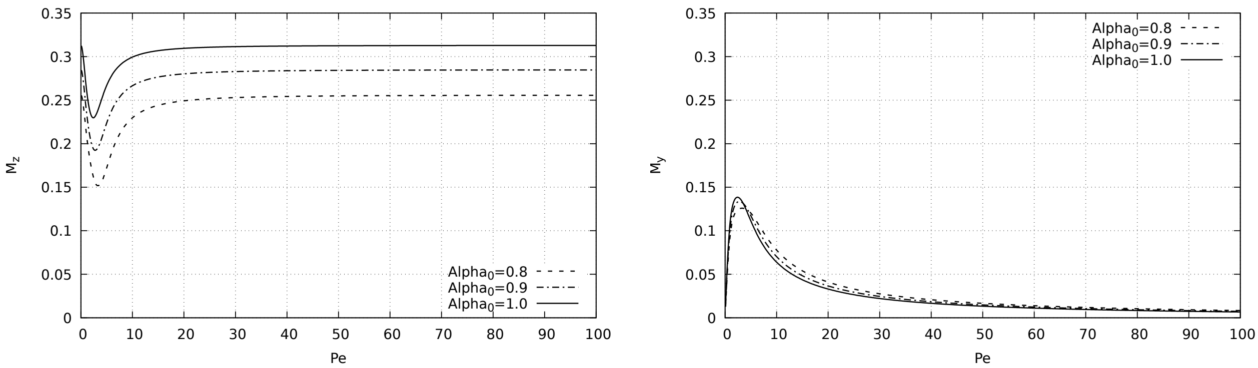

(a) M_z (b) M_y

Figure 7. Saturation limits as function of Pe for diverse α_0

4.3 THE INFLUENCE OF DIPOLAR INTERACTIONS IN STATIONARY MAGNETIC AND SHEAR FIELDS

The last step in the analysis of a stationary excitation is the full model with the incorporation of interparticle correlations according to the model of Ivanov and Kuznetsova, 2001. This variation of Shliomis's model takes place in the equilibrium magnetization $\boldsymbol{M_0}$ through the parameter λ. Considering $\lambda \neq 0$ the long range particle interactions are modeled by this third order asymptotic theory through equations 2, 3, 4, 5 and 6. In this context the volume fraction of magnetic particles ϕ also takes place and can be explored.

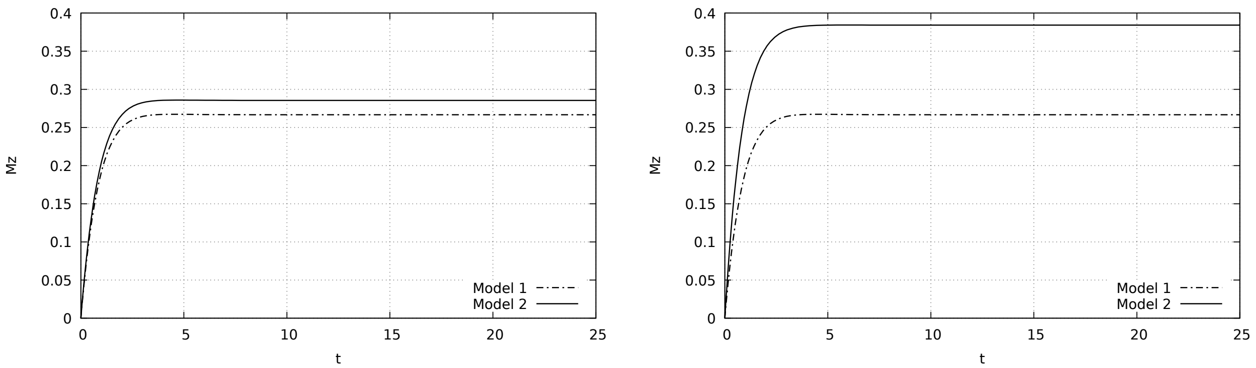

(a) $\phi = 0.01$ (b) $\phi = 0.10$

Figure 8. Comparison between models for the following input parameters: $\alpha_0 = 1$, $Pe = 1$ and $\lambda = 1$. Model 2 neglects dipolar interactions (Langevin model to compute M_0) and model 3 consideres interparticle correlations (Ivanov and Kuznetsova model to compute M_0).

Figure 8 indicates that the result of particle interactions increases the magnetization saturation limit, what can be understood as an increase of the effective applied magnetic field. This is a clear example of collective behavior in the realm of the suspension micro-structure. The intensity of this effect can be changed through the parameters λ and ϕ, the first one affects the ratio between this interaction and the Brownian energy and the second one intensifies the effect of particle interactions.

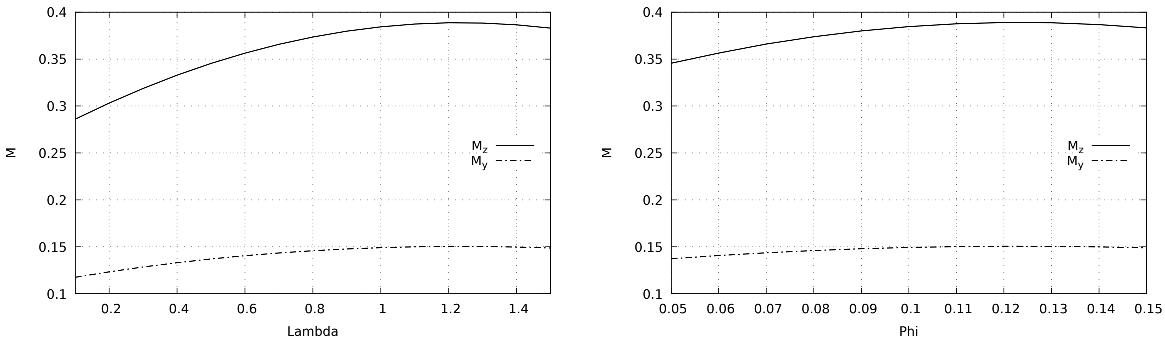

(a) Influence of λ in magnetization saturation limit. (b) Influence of ϕ in magnetization saturation limit.

Figure 9. Influences of dipoles interactions for the following group of parameters: $Pe = 1$ and $\alpha_0 = 1$.

4.4 RELAXATION MODEL WITH OSCILLATING MAGNETIC FIELD

Now we turn back our attention to the first model explored here (the relaxation term balancing the magnetization time derivative), worth mention that the equilibrium magnetization $\boldsymbol{M_0}$ also becomes oscillating in this configuration. Here we do not consider the influence of the restorative magnetic torques nor the shear rate term. The time series of magnetization, showed in Fig. 10(a), shows a periodic behavior, according to the input excitation, and the phase-space diagram, represented in Fig. 10(b), shows the existence of a singular frequency of oscillation. Here we have neglected the restorative magnetic torques, for this reason we have no coupling between M_y and M_z and consequently $M_y \to 0$.

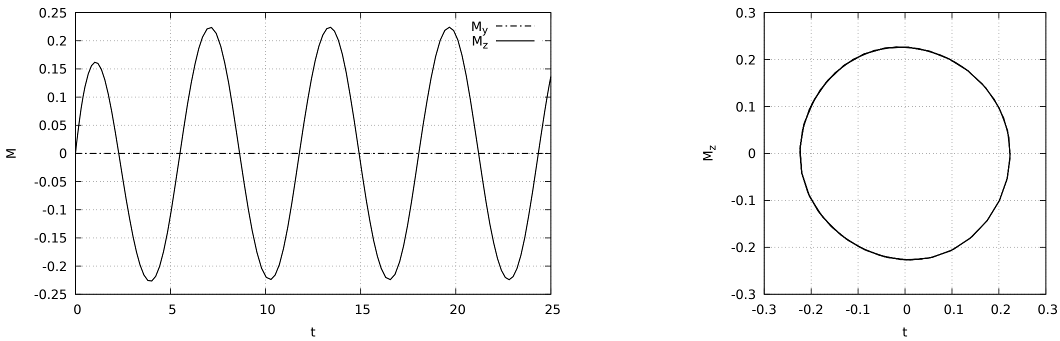

(a) Time series of magnetization for diverse Pe. (b) Phase-space diagram for $Pe = 1$.

Figure 10. Solution for magnetization using $\alpha_0 = 1$.

4.5 FULL MODEL WITH OSCILLATING MAGNETIC FIELD AND CONSTANT SHEAR-RATE

Now we inclue the effect of the restorative magnetic torques for an oscillating magnetic field and also compute the influence of a constant shear rate. It is important to mention that since in this analysis the shear rate is kept constant we can only observe a single frequency in the time series behavior. Figure 11 reveals the appearance of M_y with a little distortion in the phase-space diagram, shown in Fig. 11(b). The component M_y also seems to be out of phase with respect to M_z, as shown in Fig. 11(a).

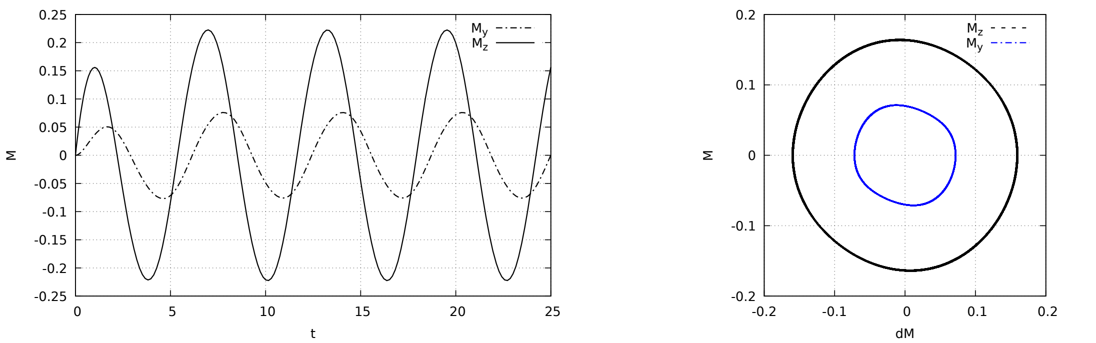

(a) Time series of magnetization for $Pe = 1$ and $\alpha_0 = 1$. (b) Phase-space diagram for $Pe = 1$ and $\alpha_0 = 1$.

Figure 11. Full model response for oscillating field with $\omega_H = 1$ and constant shear-rate.

Figure 12(a) reveals that the influence of the Peclet number seems to be quite similar to the behavior observed for the stationary field in the sense that it delays the particles perception of the resulting torques. It is possible to observe a different amplitude in the beginning of the plot, this occurs in the interval $t = [0, 4.8]$. The Peclet number also affects the amplitude of the unsteady magnetization curves. The influence of the parameter α_0 is also similar to the stationary case, affecting only the amplitude of oscillation.

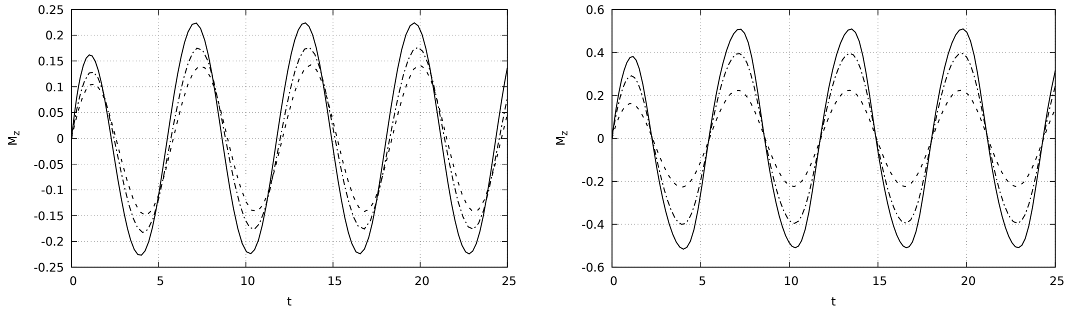

(a) Time series of magnetization for diverse Pe and $\alpha_0 = 1$. (b) Phase-space diagram for $Pe = 1$ and diverse α_0.

Figure 12. In Fig.12(a) the full line stands for the solution with Pe=1.0, the dash-dotted line for Pe=1.5 and the dash line for Pe=2.0.

4.6 FULL MODEL WITH OSCILLATING MAGNETIC FIELD AND SHEAR RATE

With the insertion of an oscillating shear rate, the physical model is complete. However it is worth mention that in this analysis we neglect the effect of particle interaction in the equilibrium magnetization M_0. In this configuration the frequencies of excitation, $\omega_{\dot{\gamma}}$ and ω_H, are combined in different ways as showed in Fig. 13.

An interesting feature of this model is that the anisotropic behavior of the applied field (in the z direction) suppresses the influence of the oscillatory shear in the magnetization response in the direction of the field. However, the perpendicular component M_y is strongly affected by the combined effect of an oscillatory magnetic field and shear rate.

We can also notice that the decrease of the shear frequency increases the nonlinear behavior of M_y. We note three limit circles in the phase-space diagram for $\omega_{\dot{\gamma}} = 0.5$, but the M_z component presents a dynamic oscillatory behavior with only one energy level. This behavior changes for $\omega_{\dot{\gamma}} = 0.2$ as we note an energy spreading the behavior of M_z in the phase-space diagram. As we increase the frequency of the shear the behavior tends to be more linear, although still harmonic off course. The increase of $\omega_{\dot{\gamma}}$ also decreases the oscillation amplitude of M_y and M_z.

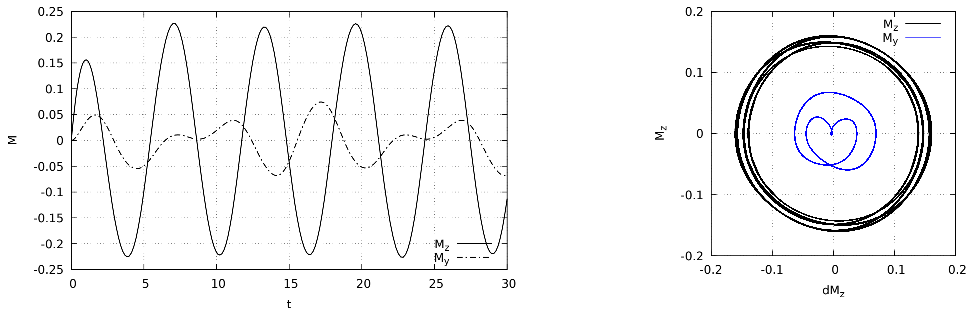

(a) Time series of magnetization for $\omega_{\dot{\gamma}} = 0.2$ and $\omega_H = 1.0$. (b) Phase-space diagram for $\omega_{\dot{\gamma}} = 0.2$ and $\omega_H = 1.0$.

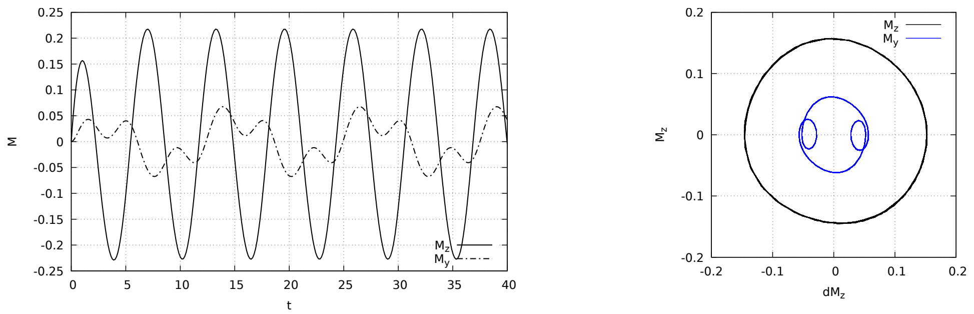

(c) Time series of magnetization for $\omega_{\dot{\gamma}} = 0.5$ and $\omega_H = 1.0$. (d) Phase-space diagram for $\omega_{\dot{\gamma}} = 0.5$ and $\omega_H = 1.0$.

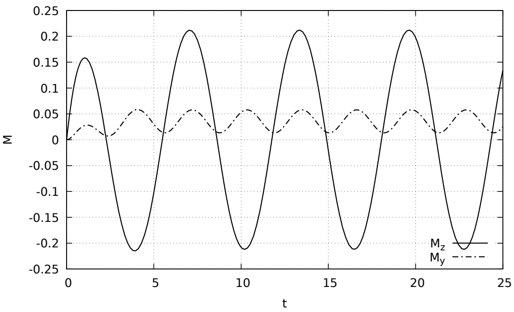

(e) Time series of magnetization for $\omega_{\dot{\gamma}} = 1.0$ and $\omega_H = 1.0$.

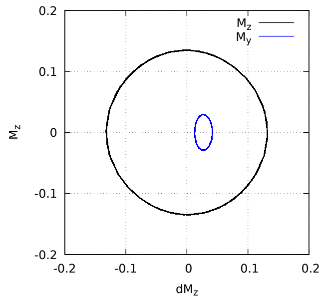

(f) Phase-space diagram for $\omega_{\dot{\gamma}} = 1.0$ and $\omega_H = 1.0$.

Figure 13. Solution for magnetization using the full model with an oscillating magnetic field and shear rate for $Pe = 1$ and $\alpha_0 = 1$.

A very interesting feature is that $\omega_{\dot{\gamma}}$ also affects the frequencies in which energy is storage in the system. Figures 14 show the FFTs for the same cases explored in figure 13. It is important to notice that the magnetization component in the direction of the field storages the energy of the oscillatory magnetic field in its frequency and is only slightly affect by the frequency of the shear. A very small amount of energy is stored by M_z in other frequencies different from ω_H. However, the influence of the combined effect of the frequencies of the magnetic and shear fields are strongly perceived by the component M_y. It is also interesting to notice that the higher energetic levels of M_y occur in frequencies around ω_H. We also observe an interesting tendency of the frequencies were energy is manifested in the oscillatory behavior of M_y. Note that the frequency peaks for M_y occur in the frequencies $\omega = \omega_H \pm \omega_{\dot{\gamma}}$.

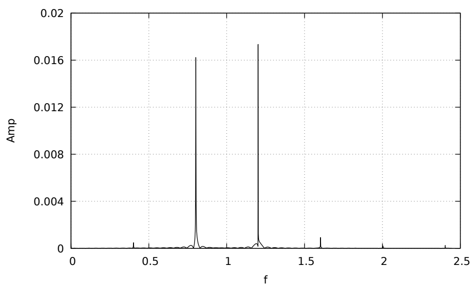

(a) M_y with $\omega_{\dot{\gamma}} = 0.2$ and $\omega_H = 1.0$.

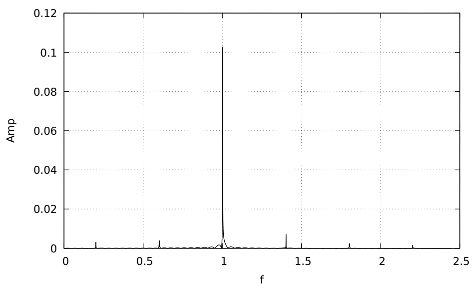

(b) M_z with $\omega_{\dot{\gamma}} = 0.2$ and $\omega_H = 1.0$.

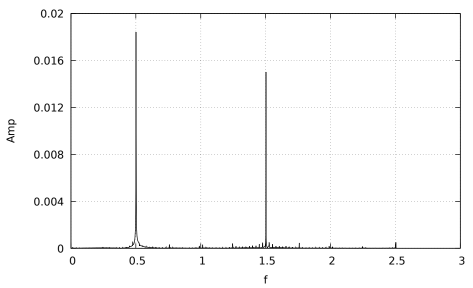

(c) M_y with $\omega_{\dot{\gamma}} = 0.5$ and $\omega_H = 1.0$.

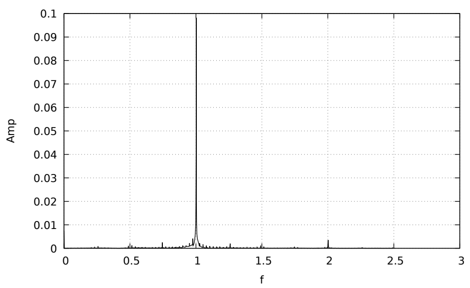

(d) M_z with $\omega_{\dot{\gamma}} = 0.5$ and $\omega_H = 1.0$.

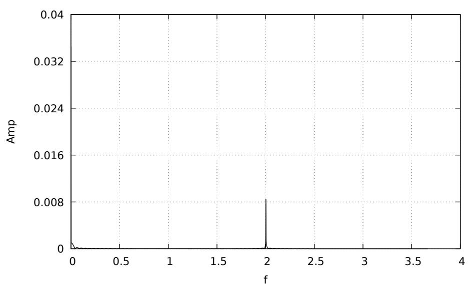

(e) M_y with $\omega_{\dot{\gamma}} = 1.0$ and $\omega_H = 1.0$.

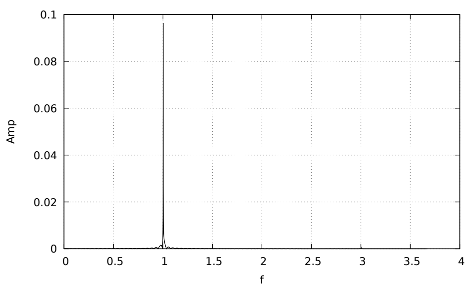

(f) M_z with $\omega_{\dot{\gamma}} = 1.0$ and $\omega_H = 1.0$.

Figure 14. FFTs for magnetization using the full model with an oscillating magnetic field and shear rate for $Pe = 1$ and $\alpha_0 = 1$.

5. CONCLUDING REMARKS

This work explored all the known physical mechanisms in the phenomenological magnetization equation proposed in the early 70s by Shiliomis (1971). We have shown how each physical mechanism acts in order to rule the magnetization dynamics of ferrofluids. The comprehension of these mechanisms is fundamental to the closure of the continuum balance equations of Ferrohydrodynamics. We have observed how the physical parameters of the problem influence the magnetization dynamics for both stationary and oscillatory magnetic and shear fields. The most remarkable behavior was observed for the full model with both (magnetic and shear) oscillatory fields. We have noticed a highly nonlinear magnetization behavior, specially for the component perpendicular to the magnetic field. We have also observed the necessity of a 3D treatment for $Pe \gg 1$ for stationary fields. A proposal of future works is the 3D treatment of the problem in order to capture the physics that could not be observed in this 2D approach.

6. AKNOWLEDGMENTS

The authors wish to acknowledge the support of this work by FAPESP-Brazil under the grant number 2017/05643-8.

7. REFERENCES

Cunha, F. R., Abade, G. C., Souza, A. J. e Hinch E. J., 2002, Modeling and Direct Simulation of Velocity Fluctuations and Particle-Velocity Correlations in Sedimen- tation, Journals of Fluids Engineering, Vol. 124, pp-957-968.

Cunha, F.R., Sobral, Y.D. e Gontijo, R.G., 2013, Stabilization of concentration waves in fluidized beds of magnetic particles, Powder Technology, Elsevier, pp 219-229.

Ivanov, A. O. e Kuznetsova, O. B., 2001, Magnetic properties of dense ferrofluids: An influence of interparticle correlations, Physical Review E, Vol. 64, 041405.

Larson, R.G.: The structure and rheology of complex fluids. Oxford University Press, New York (1999) 250, 257, 259, 261, 268, 270, 293.

Lüubbe, A. S., Alexiou, C. e Bergemann C., 2001,Clinical Applications of Magnetic Drug Targering, Journal of Surgical Research, Vol. 95, pp. 200-206.

McTague, J.P.: Magnetoviscosity of magnetic colloids. J. Chem. Phys. 51, 133- 136 (1969) 250, 252.

Odenbach, S., Müller, H.W.: Stationary off equilibrium magnetization in ferrofluids under rotational and elongational flow. Phys. Rev. Lett.

Odenbach, S., 2009, Colloidal Magnetic Fluids: Basics, Development and Application of Ferrofluids, Springer-Verlag Berling Heidelberg, ISBN: 978-3-540-85386-2.

Raj, K., Moskowitz, B., Casciari, R.: Advances in ferrofluid technology. J. Magn. Magn. Mater. 149, 174-180 (1995) 249. Rosensweig, R. R., Kaiser, R., and Misckolczy, G. 1969. Viscosity of magnetic fluid in a magnetic field. J. Colloid Interface Sci. 29 (4), 680-6.

Rosensweig, R. E., 2014. *Ferrohydrodynamics*. Dover Publications Inc, New York, 2nd edition.

Snyder, S. M., Cader, T. e Finlayson, B. A., 2002, Finite Element Model of Magneto- convection of a Ferrofluid, Journal of Magnetism and Magnetic Materials, Article in Press.

Shliomis, M.I.: Effective viscosity of magnetic suspensions. Sov. Phys. JETP 34(6), 1291-1294 (1972) 250, 251.

Sobral, Y. D., 2004, Estabilidade hidrodinâmica e magnética de leitos fluidizados, Dissertação de Mestrado, Publicação DM-73, Departamento de Engenharia Mecãnica, Universidade de Brasília, Brasília, DF, 286 p.

Voltairas, P. A., Fotiadis, D. I. e Michalis, L. K., 2002, Hydrodynamics of Magnetic Drug Targering, Journal of Biomechanics, Vol. 35, pp. 813-821.

8. RESPONSIBILITY NOTICE

The authors are the only responsible for the printed material included in this paper.